

Oligomers of heat-shock proteins: Structures that don't imply function

William M. Jacobs,* Tuomas P. J. Knowles, and Daan Frenkel

Department of Chemistry, University of Cambridge, Lensfield Road, Cambridge CB2 1EW, United Kingdom

(Dated: August 29, 2018)

Most proteins must remain soluble in the cytosol in order to perform their biological functions. To protect against undesired protein aggregation, living cells maintain a population of molecular chaperones that ensure the solubility of the proteome. Here we report simulations of a lattice model of interacting proteins to understand how low concentrations of passive molecular chaperones, such as small heat-shock proteins, suppress thermodynamic instabilities in protein solutions. Given fixed concentrations of chaperones and client proteins, the solubility of the proteome can be increased by tuning the chaperone-client binding strength. Surprisingly, we find that the binding strength that optimizes solubility while preventing irreversible chaperone binding also promotes the formation of weakly bound chaperone oligomers, although the presence of these oligomers does not significantly affect the thermodynamic stability of the solution. Such oligomers are commonly observed in experiments on small heat-shock proteins, but their connection to the biological function of these chaperones has remained unclear. Our simulations suggest that this clustering may not have any essential biological function, but rather emerges as a natural side-effect of optimizing the thermodynamic stability of the proteome.

Passive molecular chaperones inhibit the aggregation of cytosolic proteins and are thus a nearly ubiquitous component of living cells (1–3). Included in this class of chaperones are the small heat-shock proteins (sHSPs), which promote tolerance to a wide range of cellular stressors, such as elevated temperatures and hazardous non-specific interactions. These chaperones cannot by themselves fold or refold misassembled proteins and do not require ATP to function. Instead, passive chaperones associate reversibly with aggregation-prone proteins. Even when present in sub-stoichiometric ratios with their client proteins, sHSPs and similar chaperones are effective at suppressing aggregation and coping with environmental stress (4–6). Yet the mechanism by which this class of chaperones stabilizes the cytosol is not well understood despite significant efforts at determining the structural properties of these molecules.

In this paper, we propose that passive chaperones function by increasing the overall solubility of the proteome. Through this mechanism, passive chaperones reduce the fraction of toxic oligomers in solution and suppress the nucleation of protein aggregates. It has recently become apparent that sHSPs can also interact with protein aggregates in order to curtail further protein deposition (7–9). These aggregates are often detrimental to cellular survival, in part because they can sequester other crucial proteins (10). Here we provide simulation evidence that this effect on the proteome solubility is a generic feature of passive chaperones that associate promiscuously and reversibly with their clients.

There is substantial experimental evidence that sHSPs interact promiscuously with client proteins in chemical equilibrium. Both the rate of client aggregation and the

fraction of sHSPs associated with insoluble proteins are concentration-dependent (1, 3). Furthermore, chaperone binding responds directly to increases in the available client binding surfaces, including hydrophobic regions of destabilized clients that are only transiently exposed (11). The binding of sHSPs also modifies the size and structure of amorphous aggregates, often leading to smaller soluble clusters in which the putative chaperone binding sites are associated with the hydrophobic interfaces of the client proteins (12–14). On the basis of these dynamic chaperone-client aggregates, previous studies have suggested that such aggregates might serve as a relatively inert depot of misfolded proteins during cellular stress (2, 15–18).

However, client proteins are not the only substrates to which sHSPs bind: these chaperones are commonly found associated in polydisperse, chaperone-only oligomers both *in vitro* and *in vivo* (5, 12–14, 19–22). Recent experiments indicate that these dynamic chaperone-only oligomers are also under thermodynamic control (13, 14, 23, 24) and vary with the experimental conditions, such as the temperature and the ionic strength of the solution (23, 25, 26). Because this tendency to form oligomers is conserved across the family of sHSPs and similar molecular chaperones, it has long been recognized that dynamic fluctuations in the oligomeric state play an important role in the organization of many passive chaperones (5, 23, 27). At present, however, it is unclear whether the formation of chaperone oligomers is a key *functional* event. In fact, there is considerable evidence to the contrary: experiments have shown that mutations and post-translational modifications that alter the tendency of chaperones to form oligomers do not necessarily affect their function (25, 28–31). These observations raise the question of how, if at all, the presence of sHSP oligomers contributes to their ability to solubilize aggregation-prone proteins *in vivo*. Here we show that both the function and oligomerization of passive

* Present address: Department of Chemistry and Chemical Biology, Harvard University, 12 Oxford Street, Cambridge, MA, 02138, USA

molecular chaperones can be explained by identifying the optimal conditions for a thermodynamically stable solution of chaperones and aggregation-prone proteins. Our results suggest that low concentrations of promiscuous chaperones are a generic means of stabilizing a biological mixture with respect to a variety of nonfunctional interactions.

RESULTS

To understand how passive molecular chaperones affect the thermodynamic stability of a protein solution, we consider a minimal model of two species in solution: an aggregation-prone protein and a simple molecular chaperone. Aggregation of the client proteins is primarily driven by highly directional interactions. These interactions are mediated by ‘patches,’ which represent primarily hydrophobic regions that are commonly involved in both functional and aberrant protein–protein interactions. Chaperone–client recognition is also driven by these directional associations between chaperone monomers and the exposed patches of client monomers. Both the chaperone and client proteins may also associate via weak nonspecific interactions, which we assume to be averaged over the relative orientations of the monomers. This interaction accounts for weak and transient associations between proteins in a crowded environment (32). In this model, we do not explicitly model the overwhelming majority of proteins that are also assumed to experience the weak nonspecific interaction but are not prone to aggregation via directional interactions, as this simplification does not qualitatively affect our analysis.

Lattice model of a chaperone–client mixture

In protein solutions under physiological conditions, the interactions between proteins are short-ranged in comparison to the size of the monomers, since the high ionic strength characteristic of physiological media leads to an effective screening of electrostatic interactions (33). It is therefore appropriate to model protein interactions through nearest-neighbor contacts on a three-dimensional lattice, where unoccupied lattice sites represent an implicit solvent. Monomers interact if they reside on adjacent lattice sites, and they are free to rotate and to move among lattice sites in accordance with the equilibrium Boltzmann distribution. We assume that both the chaperone and the aggregation-prone state of the protein exist in a single coarse-grained conformation and that the interactions between proteins are determined by effective binding free energies. This coarse-graining of the internal degrees of freedom allows us to capture the effects of the intermolecular forces in a reduced set of parameters. Such an approach is particularly applicable to globular proteins in near-native states and misassembled

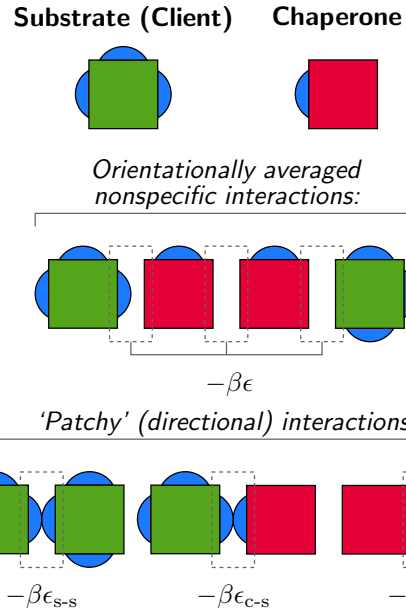


FIG. 1. A minimal model of an associating fluid of passive chaperones and aggregation-prone client proteins. Chaperone and client monomers interact via nearest-neighbor interactions on a three-dimensional cubic lattice. Orientationally averaged nonspecific interactions may be either attractive or repulsive. Directional interactions between specific binding sites, indicated by blue patches, depend on the relative orientations of the monomers and are always attractive.

proteins with hydrophobic regions that are exposed to the solution. Importantly, this lattice model is the simplest representation of a solution of associating proteins that exhibits a thermodynamic instability.

All monomers experience an orientationally averaged nonspecific interaction, which is assigned a dimensionless free energy of $-\beta\epsilon$ (Figure 1). (All interaction energies are expressed in thermal units: $\beta^{-1} \equiv k_B T$, k_B is the Boltzmann constant and T is the absolute temperature.) Aggregation-prone proteins are likely to participate in directional protein–protein interactions via multiple binding sites (1, 34–36), which also promote interactions with sHSPs (37, 38). Since we are interested in the thermodynamic consequences of this dangerous subset of cytosolic proteins, we choose a client model with three patches, which is susceptible to aggregation by means of directional interactions alone (39). The directional interactions between client monomers are assigned an attractive free energy of $-\beta\epsilon_{s-s}$ (Figure 1). These interactions are chosen to be strong enough to form insoluble client aggregates in the absence of both chaperones and additional nonspecific interactions (39).

A minimal model of a passive chaperone must be capable of binding exposed patches on the client monomers. Here we assume that the chaperone monomers have a single binding site and that the interaction free energy between chaperone and client patches is $-\beta\epsilon_{c-s}$ (Figure 1). While this assumption is clearly a simplifica-

tion of the structure of sHSPs, which may interact with diverse clients via different binding sites, this representation captures the passivation of interactive client binding sites through the burial of hydrophobic surfaces. Most critically, this representation has the physical features that are necessary to capture the qualitative effects of passive chaperones on the thermodynamics of a complex fluid.

We calculate the miscibility limit of this model, i.e., the point at which the chaperone-client mixture becomes unstable with respect to aggregation and/or demixing, using Monte Carlo simulations and finite-size-scaling techniques (see Methods). In general, a thermodynamic instability may have contributions from both directional interactions, which cause the polymerization and demixing of the strongly interacting species, and orientationally averaged interactions, which drive the formation of thermodynamic phases with differing protein densities (39). Strong directional interactions between the client proteins can thus lead to the formation of disordered aggregates and an accompanying loss of solubility. Furthermore, since the free-energy barrier separating the aggregated and protein-depleted phases vanishes at this point, large fluctuations in the protein concentration can assist the nucleation of clusters of aggregation-prone proteins. Because sHSPs are known to function at low concentrations, we assume that there are always fewer chaperones than client binding sites. In what follows, the relative amounts of the chaperone and client monomers in solution are indicated by x_c and x_s , respectively, such that $x_c + x_s = 1$.

Passive chaperones enhance the thermodynamic stability of a protein solution

Unsurprisingly, the presence of chaperones inhibits the formation of client oligomers by competing for binding to patches on the client monomers. However, this passivation of directional interactions is not the only effect of chaperone binding: the interactions between chaperones and client proteins simultaneously increase the strength of orientationally averaged nonspecific interactions that the solution can tolerate while remaining thermodynamically stable. This effect can be seen in Figure 2, which plots the miscibility limit, $\beta\epsilon^*$, at which insoluble aggregates first appear in the solution. When the strength of the orientationally averaged nonspecific interactions increases beyond this limit, i.e., $\beta\epsilon > \beta\epsilon^*$, the solution becomes unstable with respect to small fluctuations in the protein concentrations. Increasing the strength of these nonspecific interactions can thus cause the solution to become unstable without altering the strength of the directional interactions that drive the polymerization of the client monomers. Our calculations show that passive chaperones dramatically affect the miscibility limit by inhibiting polymerization and solubilizing transient clusters of client proteins, despite the fact that there are far

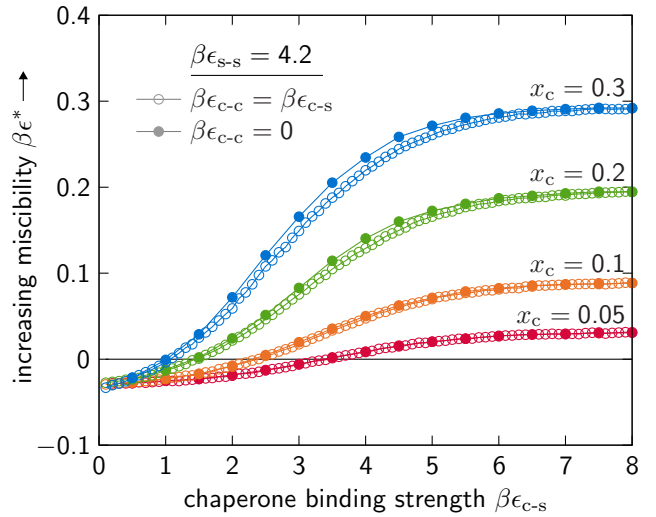


FIG. 2. The miscibility limit, $\beta\epsilon^*$, of a chaperone-client mixture depends on the chaperone-client binding strength, $\beta\epsilon_{c-s}$, and the chaperone stoichiometric fraction, x_c . The chaperone-chaperone interactions have only a minor effect on $\beta\epsilon^*$: the miscibility limits of solutions with promiscuous chaperone interfaces, for which $\beta\epsilon_{c-c} = \beta\epsilon_{c-s}$, are indicated by open circles, while the miscibility limits of solutions in which chaperone-chaperone interactions are prevented are indicated by closed circles. The client-client interaction strength, $\beta\epsilon_{s-s}$, is sufficient to drive the aggregation of clients in the absence of chaperones.

fewer chaperones than there are client binding sites.

In the absence of chaperones, i.e., $x_c \rightarrow 0$, the solution is unstable due to the strong directional interactions between the aggregating client monomers. In this case, $\beta\epsilon^*$ is negative, indicating that a solution of sufficiently concentrated client proteins in a well-screened solvent will form insoluble aggregates. It is important to note that even when $\beta\epsilon_{c-s} = 0$, the chaperones still interact nonspecifically with the client monomers through the orientationally averaged interaction $\beta\epsilon$. Here we find that the addition of such ‘inert’ chaperones has a negligible effect on the miscibility limit relative to a client-only solution. This observation implies that the majority of cytosolic proteins that are not aggregation-prone do not significantly affect the miscibility limit when the dominant instability is driven by strong directional interactions.

Our calculations further indicate that the thermodynamic forces driving these instabilities are qualitatively different in solutions with weakly and strongly binding chaperones. In the case of weakly binding chaperones ($\beta\epsilon_{c-s} \ll \beta\epsilon_{s-s}$), the solution demixes into client-enriched and client-depleted phases primarily as a result of directional interactions. Insoluble client aggregates recruit monomers via the formation of directional contacts and exchange small oligomers with the coexisting solution. With strongly binding chaperones ($\beta\epsilon_{c-s} \gg \beta\epsilon_{s-s}$), the solution forms a high-density condensate consisting of both chaperones and client proteins bound by nonspecific interactions. Under these conditions, the proteins in both

the soluble and insoluble phases exist as amorphous clusters that decrease in size as the stoichiometric ratio x_c/x_s is increased. The introduction of strongly binding chaperones, even in low concentrations, significantly increases the solution miscibility limit towards the theoretical maximum for this model, $\beta\epsilon_{\max}^* \simeq 0.87$.

Chaperone–chaperone interactions do not significantly affect the miscibility limit

Because a chaperone that interacts with a variety of clients is very likely to engage in promiscuous interactions, it is reasonable to assume that chaperones do not distinguish among the various hydrophobic surfaces in solution. The strength of interactions between chaperone binding sites is thus likely to be similar to the strength of interactions between chaperones and clients. For this reason, it is natural to assume that $\beta\epsilon_{c-c} = \beta\epsilon_{c-s}$. However, if we instead prevent chaperone–chaperone binding by setting $\beta\epsilon_{c-c} = 0$, we find that the effect on the solution miscibility limit is negligible (Figure 2).

Since the parameter $\beta\epsilon_{c-c}$ directly controls the probability of chaperone dimerization, our calculations suggest that the formation of chaperone oligomers has a very minor effect on chaperone function. Experimentally, the relationship between oligomerization and chaperone function has been probed by modifying or truncating sHSPs (25, 29–31). In agreement with the results of our calculations, the available experimental evidence indicates that alterations to the putative client binding sites on sHSPs affect the oligomer equilibria and the functionality of the chaperones independently.

A biological fitness function suggests conditions for optimized chaperone operation

Putting these results into context, we now ask, “Is there an optimal chaperone–client binding strength for a biological mixture?” Figure 2 shows that strongly binding chaperones are best suited for increasing the miscibility limit. In this case, producing more chaperones (or reducing the total concentration of aggregation-prone clients) increases $\beta\epsilon^*$ in an approximately linear relationship, allowing an organism to respond effectively to an increase in nonspecific interactions. Nevertheless, strong promiscuous interactions come at a cost: nearly irreversible binding between a chaperone and any available association site, including other proteins that are not explicitly modeled in our simulations, sequesters both interfaces, thereby preventing their participation in further functional interactions. The optimal chaperone binding strength must balance these competing requirements for solution stability and reversible binding.

Despite the complexity of naturally occurring protein solutions, we can formulate a prediction for the optimal chaperone binding strength by considering a generic bi-

ological fitness function, which quantifies the trade-offs in biological costs and benefits. Here the benefit is the increased miscibility limit, $\beta\epsilon^*$, which we have already shown is a function of both $\beta\epsilon_{c-s}$ and x_c . Any reasonable biological fitness function \mathcal{F} must satisfy $\partial\mathcal{F}/\partial\beta\epsilon^* > 0$. One potential cost arises from the sequestration of functional proteins (which are not explicitly modeled in our simulations but must be present in a naturally occurring protein solution) due to the promiscuous binding of chaperones. Another potential cost is associated with the production of chaperone molecules. These costs imply that \mathcal{F} should satisfy both $\partial\mathcal{F}/\partial\beta\epsilon_{c-s}|_{\beta\epsilon^*} < 0$ and $\partial\mathcal{F}/\partial x_c|_{\beta\epsilon^*} < 0$, respectively. Taking the total derivative of \mathcal{F} with respect to both $\beta\epsilon_{c-s}$ and x_c , we find that this fitness function is maximized where

$$\frac{\partial\beta\epsilon^*}{\partial\beta\epsilon_{c-s}} = \frac{-\frac{\partial\mathcal{F}}{\partial\beta\epsilon_{c-s}}\Big|_{\beta\epsilon^*}}{\frac{\partial\mathcal{F}}{\partial\beta\epsilon^*}} \quad \text{and} \quad \frac{\partial\beta\epsilon^*}{\partial x_c} = \frac{-\frac{\partial\mathcal{F}}{\partial x_c}\Big|_{\beta\epsilon^*}}{\frac{\partial\mathcal{F}}{\partial\beta\epsilon^*}}.$$

All partial derivatives of \mathcal{F} depend on the precise nature of the biological system and thus cannot be determined precisely. However, we can interpret the ratios of the derivatives in each of these equations as the importance of each cost relative to the benefit of stabilizing the protein solution (40). If we therefore assume, as argued above, that promiscuous chaperone binding and chaperone production are indeed significant biological costs, then these equations imply that we should seek to maximize the response functions $\partial\beta\epsilon^*/\partial\beta\epsilon_{c-s}$ and $\partial\beta\epsilon^*/\partial x_c$.

More intuitively, maximizing these response functions directs the optimal chaperone design towards the region of parameter space in which the solution miscibility limit is most sensitive to small increases in either the chaperone–client binding strength or the number of chaperone molecules in solution. The first condition, $\partial\beta\epsilon^*/\partial\beta\epsilon_{c-s}$, biases the optimal chaperone design away from values of $\beta\epsilon_{c-s}$ for which the miscibility limit increases asymptotically, thus discriminating against excessively strong binding between chaperones and clients. The second condition, $\partial\beta\epsilon^*/\partial x_c$, requires that the miscibility limit be sensitive to changes in the chaperone stoichiometric fraction.

Our calculations show that it is indeed possible to satisfy both conditions simultaneously. In Figures 3a and 3b, we plot the calculated response functions $\partial\beta\epsilon^*/\partial\beta\epsilon_{c-s}$ and $\partial\beta\epsilon^*/\partial x_c$, in dimensionless units, as functions of the chaperone stoichiometric fraction and the chaperone binding strength. We identify a ‘design window’ for optimal chaperone operation by finding the approximate range of chaperone binding strengths over which both response functions are maximized given a fixed chaperone stoichiometric fraction. The region of parameter space in which both response functions can be maximized is relatively narrow, suggesting that optimized passive chaperones should have tightly constrained binding strengths. We further find that the optimal range of chaperone binding strengths is only weakly dependent on the chaperone

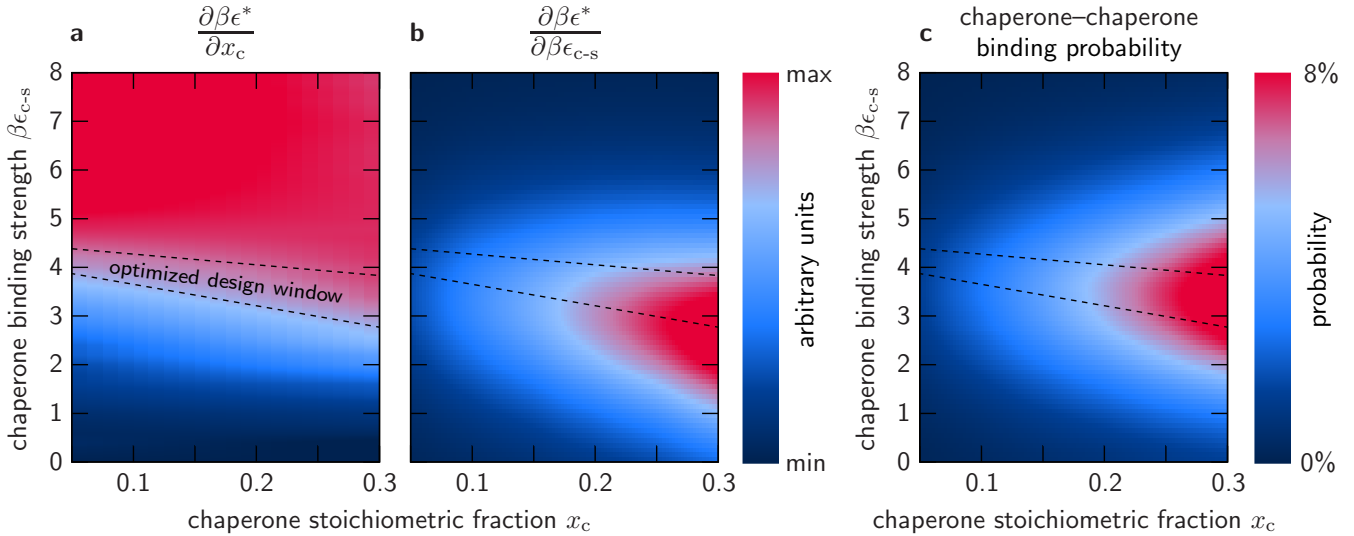


FIG. 3. The optimized design window for a passive molecular chaperone coincides with the conditions under which chaperone oligomerization is most probable. (a) The response in the solution miscibility limit to an increase in the chaperone stoichiometric fraction. The approximately linear response regime for strong binding chaperones is indicated in red. (b) The response in the solution miscibility limit to an increase in the chaperone-client binding strength. (c) The probability that a chaperone binding interface is bound to another chaperone monomer. For a given stoichiometric ratio of chaperones and clients, this probability is greatest in approximately the same design window in which both $\partial\beta\epsilon^*/\partial x_c$ and $\partial\beta\epsilon^*/\partial\beta\epsilon_{c-s}$ are simultaneously maximized.

stoichiometric fraction. This observation implies that chaperones with fixed binding strengths operate close to optimality over a wide range of sub-stoichiometric concentrations. Finally, we note that the optimal chaperone binding strength is generally weaker than the client-client interactions, indicating that the chaperones need not out-compete the aggregation-prone clients for association with exposed binding interfaces.

The optimal chaperone-client binding strength promotes chaperone oligomerization

Remarkably, our simulations reveal that the probability of finding chaperone oligomers is also highest in the region of parameter space where the optimal design conditions for chaperone activity are satisfied. In Figure 3c, we plot the probability of chaperone-chaperone binding at the miscibility limit, assuming that $\beta\epsilon_{c-c} = \beta\epsilon_{c-s}$. We find that this probability is maximal in the window of optimal chaperone binding strength over the complete range of simulated chaperone stoichiometric fractions. Under these conditions, a significant fraction of the chaperone binding sites are not associated with the aggregation-prone interfaces on the client proteins, but are rather buried in chaperone-only oligomers. This fraction may be even higher in the miscible fluid or in the presence of client proteins that are less prone to aggregation (41).

These calculations provide further evidence that the assembly of chaperone oligomers does not play a functional role. Although the choice of $\beta\epsilon_{c-c}$ affects the magnitude of the effect plotted in Figure 3c, we empha-

size that simply allowing chaperone-chaperone binding does not imply that chaperone-only oligomers will be observed at the miscibility limit: there is a large region of parameter space over which this probability is very small. In fact, for all reasonable choices of $\beta\epsilon_{c-c}$, i.e., $0 < \beta\epsilon_{c-c} \lesssim \beta\epsilon_{c-s}$, the outcome shown in Figure 3c is qualitatively unchanged. Our simulations thus indicate that the ability to assemble chaperone oligomers affects neither the anti-aggregation function of the chaperones nor their adherence to the proposed design constraints.

DISCUSSION

We have shown that a simple model of chaperone-client mixtures reveals two generic and unexpected features of passive molecular chaperones. First, chaperone-chaperone interactions only marginally affect the stability of a protein solution in which strong directional interactions drive the aggregation of client proteins. Second, promiscuous passive chaperones tend to assemble chaperone oligomers under conditions where the chaperone-client binding strength balances the requirement for proteome stability with the need to avoid irreversible binding. Taken together, these results suggest that the assembly of oligomers of passive molecular chaperones is not an essential functional event for stabilizing a protein solution. Instead, this behavior emerges as a side-effect of operating under thermodynamically optimal conditions.

In order to arrive at this conclusion, we have proposed that passive chaperones perform their anti-aggregation function by increasing the miscibility limit of a protein

solution. Through this mechanism, passive chaperones inhibit the sequestration of functional proteins and increase the thermodynamic stability of a biological mixture with respect to random nonspecific interactions. Importantly, our simulations demonstrate that this mechanism is physically plausible even when the aggregation-prone client proteins greatly outnumber the chaperones. We emphasize that only the ratio of chaperone molecules to client binding interfaces, not the total concentration of chaperones in solution, is relevant for chaperone function. In all cases considered here, the stoichiometric fraction of chaperones is much lower than $x_c = 0.75$, the fraction that would be required to passivate all binding sites on the three-patch client monomers in the solution. The fact that the chaperones that fulfill this anti-aggregation function are highly conserved in both lower and higher organisms suggests that there is a strong evolutionary pressure to perform this role in an optimized fashion. Our calculations indicate that the range of suitable chaperone binding strengths is indeed narrow and that the principles for an optimal design emerge from general thermodynamic arguments.

The generality of the present model suggests that the assembly of chaperone-only oligomers would not be affected by introducing additional detail in an off-lattice model. Such an extension, however, would allow a much wider variety of chaperone oligomers to be observed. The significant coarse-graining involved in the development of the present model and the high symmetry imposed by the lattice do not permit the reproduction of many structural features of sHSPs. For instance, all three domains of many sHSPs are believed to be involved in the assembly of higher-order oligomers (14, 24), while the chaperones in the present model may only form dimers through client-binding interfaces. Nevertheless, such detailed molecular interactions are unlikely to affect the physical mechanism by which passive chaperones suppress aggregation.

Most importantly, the simplicity of this model allows us to make generic predictions about the thermodynamics of passive molecular chaperones. The critical points associated with the instabilities observed in this model of chaperone-client mixtures belong to the Ising universality class. The biological relevance of this universality class, which is unaffected by the molecular-level details of the model, is supported by experiments on solutions of globular proteins (42, 43), including observations of aggregation and liquid–liquid phase separation in concentrated protein solutions (44–46). Furthermore, the nucleation of aggregated phases is also likely to be enhanced in the vicinity of a metastable critical point (47, 48). For example, recent simulations have shown that clustering through nonspecific interactions plays an important role in the kinetics of amyloid fibril nucleation (49). In addition, all protein–protein interaction free energies in this model are in the physical range of a few $k_B T$.

Although we have discussed the behavior of protein solutions precisely at the miscibility limit, these calcula-

tions provide insight into the thermodynamics of protein solutions both close to and far away from these critical conditions. In the vicinity of a critical point, fluctuations in both the protein density and the intermolecular contacts within aggregates are significant, and a broad distribution of cluster sizes is observed at equilibrium. In this sense, our calculations support the assertion that subunit exchange is essential for the function of sHSPs and related chaperones (5, 27, 50–52). Even if the aggregates are not fully equilibrated due to slow kinetics, the reduced free-energy barrier for the formation of gel-like aggregates has direct consequences for the stability of a protein solution (53). Further away from the critical point, the miscibility limit still plays an important role in determining the equilibrium thermodynamics of a protein solution. Smaller, soluble aggregates can exist in the miscible fluid, and chaperones may cluster with aggregation-prone clients, thereby maintaining their solubility. In an unstable solution beyond the miscibility limit, thermodynamic equilibrium among condensates and unbound proteins reduces the concentration of aggregation-prone clients in the surrounding fluid. Altering the overall concentration of client monomers in the mixture shifts the total number of client monomers bound in condensates without affecting the concentration of the proteins in the coexisting solution.

CONCLUSIONS

We have presented a minimal model of a mixture of passive molecular chaperones and aggregation-prone proteins. By calculating the limit of thermodynamic stability in this model protein solution, we have shown how passive chaperones that are expressed in substoichiometric ratios with their clients can substantially suppress aggregation. We have further argued that the biological costs associated with chaperone production and promiscuous, irreversible binding significantly constrain the optimal design of an effective passive chaperone. We find that if passive chaperones interact promiscuously with exposed hydrophobic surfaces, then the assembly of chaperone oligomers emerges as a nonfunctional side-effect of this thermodynamically optimal design. Because of the generality of the model, these conclusions are relevant to a broad class of molecular chaperones. Fully atomistic simulations could provide further information on the parameters governing the interaction strengths between chaperones and their aggregation-prone targets as well as between the passive chaperones themselves. Such simulations could therefore provide a means of transferring the general thermodynamic principles uncovered by the coarse-grained simulations presented here to detailed models of specific chaperone-client mixtures.

METHODS

In the lattice model considered here, the limit of thermodynamic stability of a well-mixed solution is encountered at the critical surface for phase separation. In what follows, we describe the Monte Carlo simulations and finite-size-scaling theory used to calculate points on this critical surface. Our approach is a generalization of the computational strategy described in detail in Ref. 39.

In general, the critical surface of a multicomponent mixture has dimension $d - 2$, where d is the total number of independent thermodynamic fields (54). The independent thermodynamic fields in the present model are the dimensionless chemical potentials of both the chaperones and the clients, $\beta\mu_c$ and $\beta\mu_s$, respectively, as well as the dimensionless interaction energies: $\beta\epsilon$, $\beta\epsilon_{s-s}$, $\beta\epsilon_{c-s}$ and $\beta\epsilon_{c-c}$. The relevant critical surface in this model is thus a 4-dimensional manifold.

We perform biased grand-canonical Monte Carlo simulations, as described in Ref. 39, to collect statistically independent lattice configurations near the critical surface. We use a $L \times L \times L$ cubic lattice with periodic boundary conditions and set $L = 12$ so that all simulations are carried out in the scaling regime. We then apply the finite-size-scaling theory of Wilding and Bruce (55, 56) to solve self-consistently for the critical order parameter, $\hat{\mathcal{M}}$, and the critical orientationally averaged nonspecific energy, $\beta\epsilon^*$, at fixed values of $\beta\epsilon_{s-s}$, $\beta\epsilon_{c-s}$, $\beta\epsilon_{c-c}$ and x_c . In order to determine each critical point plotted in Figure 2, we approximate the marginal probability distribution $p(\mathcal{M})$ from the grand-canonical samples and then tune this distribution in order to match the known distribution of the critical ordering operator in the three-dimensional Ising universality class, $p_{\mathcal{M}}$. This computational procedure is described below.

In a two-solute solution, with two independent dimensionless chemical potentials $\beta\mu_c$ and $\beta\mu_s$, the critical order parameter must account for fluctuations in the number densities of both the client and chaperone monomers, ρ_s and ρ_c , respectively, as well as fluctuations in the internal energy density, u . The critical fluctuations in the number densities can be described by a basis vector $\hat{\nu}$, which indicates the difference in compositions of the two incipient phases (57). We therefore define $\hat{\mathcal{M}}$ to be the linear combination

$$\hat{\mathcal{M}} \equiv \nu_s \hat{\rho}_s + \nu_c \hat{\rho}_c - s \hat{u}, \quad (1)$$

where both $\hat{\nu}$ and the field-mixing parameter s must be determined self-consistently. The grand-canonical distribution of \mathcal{M} is constructed from the simulation data according to

$$p_{\text{gc},k}^{(\mathcal{M})} \equiv \Lambda \sum_v w_v \mathbf{1} \left\{ \delta \mathcal{M}_k \leq \left[(\rho_s, \rho_c, u)_v \cdot \hat{\mathcal{M}} \right] < \delta \mathcal{M}_{k+1} \right\}, \quad (2)$$

where the index v runs over all independent samples and $\mathbf{1}\{\cdot\}$ is the indicator function. The system-dependent scaling constant Λ must be determined self-consistently.

The bin size is chosen such that $(\delta \mathcal{M}_{k+1} - \delta \mathcal{M}_k) = L^{-3}$, where $\delta \mathcal{M} \equiv \Lambda(\mathcal{M} - \mathcal{M}^*)$ and \mathcal{M}^* is the ensemble-averaged mean value of \mathcal{M} .

We then construct a χ^2 -function that seeks to minimize the difference between the observed distribution of \mathcal{M} and the universal distribution, $p_{\mathcal{M}}$, while obeying the imposed composition constraint:

$$\begin{aligned} \chi^2 \equiv & \sum_k \frac{\left[p_{\text{gc},k}^{(\mathcal{M})}(\beta \vec{f}) - p_{\mathcal{M}}(\delta \mathcal{M}_k / \Lambda) \right]^2}{\sigma_k^2} \\ & + \sum_{i \in \{s,c\}} \frac{\left(\langle \rho_i(\beta \vec{f}) \rangle / \sum_{j \in \{s,c\}} \langle \rho_j(\beta \vec{f}) \rangle - x_i \right)^2}{\sigma_i^2}, \end{aligned} \quad (3)$$

where $\beta \vec{f} \equiv (\beta\epsilon, \beta\epsilon_{s-s}, \beta\epsilon_{c-s}, \beta\epsilon_{c-c}, \beta\mu_s, \beta\mu_c)$ and the index k runs over all bins. In the second term, $\langle \rho_i \rangle$ indicates the ensemble-averaged number density of component i . We estimate the error in the sampled distribution of \mathcal{M} to be

$$\sigma_k^2 = \frac{\left(\sum_v w_v^2 \mathbf{1}_{k,v} \right) - \left(\sum_v w_v \mathbf{1}_{k,v} \right)^2 / n_{\text{samples}}}{\sum_v w_v}, \quad (4)$$

where $\mathbf{1}_{k,v}$ is the indicator function written out explicitly in Eq. (2), and we estimate the error in the observed composition at the critical point to be

$$\sigma_i^2 = \frac{1}{\phi^2} \left[\sum_{j,k \in \{s,c\}} \left(\delta_{ij} - \frac{\rho_i}{\phi} \right) \langle \delta \rho_j \delta \rho_k \rangle \left(\delta_{ik} - \frac{\rho_i}{\phi} \right) \right], \quad (5)$$

where $\langle \delta \rho_j \delta \rho_k \rangle \equiv \langle \rho_j \rho_k \rangle - \langle \rho_j \rangle \langle \rho_k \rangle$, $\phi \equiv \sum_{j \in \{s,c\}} \rho_j$ and δ_{ij} is the Kronecker delta.

Finally, we calculate the probability of chaperone dimerization, $\langle p_{c-c} \rangle$, directly from the simulation data according to the definition

$$\langle p_{c-c} \rangle^* \equiv \left\langle \frac{2n_{cc}}{N_c} \right\rangle^*, \quad (6)$$

where n_{cc} is the number of chaperone–chaperone patch contacts and N_c is the total number of chaperone monomers on the lattice. In this definition, $\langle \cdot \rangle^*$ indicates a grand-canonical average obtained at the critical point with the specified chemical potentials and directional interaction energies.

ACKNOWLEDGMENTS

W.M.J. acknowledges support from the Gates Cambridge Trust and the National Science Foundation Graduate Research Fellowship under Grant No. DGE-1143678. T.P.J.K. acknowledges support from the European Research Council, the BBSRC and the Frances and Augustus Newman Foundation.

REFERENCES

[1] R. J. Ellis, *Chaperone function: The orthodox view* (Cambridge University Press, New York, 2005).

[2] J. Tyedmers, A. Mogk, and B. Bukau, *Nat. Rev. Mol. Cell Biol.* **11**, 777 (2010).

[3] D. A. Drummond and C. O. Wilke, *Cell* **134**, 341 (2008).

[4] T. M. Treweek, A. M. Morris, and J. A. Carver, *Aust. J. Chem.* **56**, 357 (2003).

[5] J. A. Carver, A. Rekas, D. C. Thorn, and M. R. Wilson, *IUBMB Life* **55**, 661 (2003).

[6] G. K. Hochberg, H. Ecroyd, C. Liu, D. Cox, D. Cascio, M. R. Sawaya, M. P. Collier, J. Stroud, J. A. Carver, A. J. Baldwin, C. V. Robinson, D. S. Eisenberg, J. L. P. Benesch, and A. Laganowsky, *Proc. Natl. Acad. Sci. U.S.A.* **111**, E1562 (2014).

[7] S. L. Shammas, C. A. Waudby, S. Wang, A. K. Buell, T. P. J. Knowles, H. Ecroyd, M. E. Welland, J. A. Carver, C. M. Dobson, and S. Meehan, *Biophys. J.* **101**, 1681 (2011).

[8] C. A. Waudby, T. P. J. Knowles, G. L. Devlin, J. N. Skepper, H. Ecroyd, J. A. Carver, M. E. Welland, J. Christodoulou, C. M. Dobson, and S. Meehan, *Biophys. J.* **98**, 843 (2010).

[9] T. P. J. Knowles, W. Shu, G. L. Devlin, S. Meehan, S. Auer, C. M. Dobson, and M. E. Welland, *Proc. Natl. Acad. Sci. U.S.A.* **104**, 10016 (2007).

[10] N. F. Bence, R. M. Sampat, and R. R. Kopito, *Science* **292**, 1552 (2001).

[11] H. S. Mchaourab, J. A. Godar, and P. L. Stewart, *Biochemistry* **48**, 3828 (2009).

[12] M. Haslbeck, S. Walke, T. Stromer, M. Ehrnsperger, H. E. White, S. Chen, H. R. Saibil, and J. Buchner, *EMBO J.* **18**, 6744 (1999).

[13] E. Basha, H. O'Neill, and E. Vierling, *Trends. Biochem. Sci.* **37**, 106 (2012).

[14] M. Haslbeck, T. Franzmann, D. Weinfurter, and J. Buchner, *Nat. Struct. Mol. Biol.* **12**, 842 (2005).

[15] M. Arrasate, S. Mitra, E. S. Schweitzer, M. R. Segal, and S. Finkbeiner, *Nature* **431**, 805 (2004).

[16] M. Tanaka, Y. M. Kim, G. Lee, E. Junn, T. Iwatsubo, and M. M. Mouradian, *J. Biol. Chem.* **279**, 4625 (2004).

[17] F. U. Hartl, A. Bracher, and M. Hayer-Hartl, *Nature* **475**, 324 (2011).

[18] S.-H. Park, Y. Kukushkin, R. Gupta, T. Chen, A. Konagai, M. S. Hipp, M. Hayer-Hartl, and F. U. Hartl, *Cell* **154**, 134 (2013).

[19] U. Jakob, M. Gaestel, K. Engel, and J. Buchner, *J. Biol. Chem.* **268**, 1517 (1993).

[20] J. R. Thériault, H. Lambert, A. T. Chávez-Zobel, G. Charest, P. Lavigne, and J. Landry, *J. Biol. Chem.* **279**, 23463 (2004).

[21] R. Van Montfort, C. Slingsby, and E. Vierling, *Adv. Protein. Chem.* **59**, 105 (2002).

[22] A. L. Robertson, S. J. Headley, H. M. Saunders, H. Ecroyd, M. J. Scanlon, J. A. Carver, and S. P. Bottomley, *Proc. Natl. Acad. Sci. U.S.A.* **107**, 10424 (2010).

[23] G. K. Hochberg and J. L. Benesch, *Prog. Biophys. Mol. Biol.* **115**, 11 (2014).

[24] A. J. Baldwin, G. R. Hilton, H. Lioe, C. Bagnérés, J. L. Benesch, and L. E. Kay, *J. Mol. Biol.* **413**, 310 (2011).

[25] Y. Sun and T. H. MacRae, *Cell Mol. Life Sci.* **62**, 2460 (2005).

[26] X. Fu, C. Liu, Y. Liu, X. Feng, L. Gu, X. Chen, and Z. Chang, *Biochem. Biophys. Res. Commun.* **310**, 412 (2003).

[27] F. Stengel, A. J. Baldwin, A. J. Painter, N. Jaya, E. Basha, L. E. Kay, E. Vierling, C. V. Robinson, and J. L. P. Benesch, *Proc. Natl. Acad. Sci. U.S.A.* **107**, 2007 (2010).

[28] D. Hayes, V. Napoli, A. Mazurkiew, W. F. Stafford, and P. Graceffa, *J. Biol. Chem.* **284**, 18801 (2009).

[29] I. K. Feil, M. Malfois, J. Hendale, H. van der Zandt, and D. I. Svergun, *J. Biol. Chem.* **276**, 12024 (2001).

[30] M. Haslbeck, A. Ignatiou, H. Saibil, S. Helmich, E. Frenzl, T. Stromer, and J. Buchner, *J. Mol. Biol.* **343**, 445 (2004).

[31] J. A. Aquilina, J. L. Benesch, L. L. Ding, O. Yaron, J. Horwitz, and C. V. Robinson, *J. Biol. Chem.* **280**, 14485 (2005).

[32] For the purpose of this thermodynamic analysis, any sufficiently weak interaction between monomers can be modeled as a pair-wise isotropic interaction, as discussed in Ref. 39. Assuming a single value for this nonspecific interaction among all types of proteins is clearly a gross simplification of a complex multicomponent solution. Nevertheless, lattice simulations of an explicitly multicomponent mixture have shown that a single effective interaction strength can describe the phase behavior of such a mixture in the limit of a large number of components (57).

[33] J. D. Gunton and A. Shirayev, *Protein condensation: Kinetic pathways to crystallization and disease* (Cambridge University Press, 2007).

[34] A. Pastore and P. A. Temussi, *Curr. Opin. Struct. Biol.* **22**, 30 (2012).

[35] A. Cumberworth, G. Lamour, M. M. Babu, and J. Gsponer, *Biochem. J.* **454**, 361 (2013).

[36] N. S. de Groot, M. Torrent, A. Villar-Piqué, B. Lang, S. Ventura, J. Gsponer, and M. M. Babu, *Biochem. Soc. Trans.* **40** (2012).

[37] J. A. Carver, R. A. Lindner, C. Lyon, D. Canet, H. Hernandez, C. M. Dobson, and C. Redfield, *J. Mol. Biol.* **318**, 815 (2002).

[38] X. Fu, Z. Chang, X. Shi, D. Bu, and C. Wang, *Protein Sci.* **23**, 229 (2014).

[39] W. M. Jacobs, D. W. Oxtoby, and D. Frenkel, *J. Chem. Phys.* **140**, 204109 (2014).

[40] To a good approximation, we can assume that the cost-derivatives of \mathcal{F} are approximately constant. If the low-concentration chaperones bind reversibly to any exposed patch in the solution (implying $\beta\epsilon_{c-s} \lesssim \beta\epsilon_{s-s}$ in the present model), then the law of mass action implies that the cost due to promiscuous binding must be approximately linear in both the chaperone concentration and binding strength. It is also reasonable to assume that the cost associated with the production of chaperone molecules is approximately linear in the chaperone concentration.

[41] In the present model, the aggregation propensity of the client monomers can be tuned by adjusting $\beta\epsilon_{s-s}$ or by replacing the clients with the alternative three-patch model studied in Ref. 39.

[42] J. A. Thomson, P. Schurtenberger, G. M. Thurston, and G. B. Benedek, *Proceedings of the National Academy of Sciences* **84**, 7079 (1987).

[43] P. Schurtenberger, R. A. Chamberlin, G. M. Thurston,

J. A. Thomson, and G. B. Benedek, *Phys. Rev. Lett.* **63**, 2064 (1989).

[44] V. G. Taratuta, A. Holschbach, G. M. Thurston, D. Blankschtein, and G. B. Benedek, *J. Phys. Chem.* **94**, 2140 (1990).

[45] M. L. Broide, C. R. Berland, J. Pande, O. O. Ogun, and G. B. Benedek, *Proc. Natl. Acad. Sci. U.S.A.* **88**, 5660 (1991).

[46] Y. Wang, A. Lomakin, R. F. Latypov, J. P. Laubach, T. Hidemitsu, P. G. Richardson, N. C. Munshi, K. C. Anderson, and G. B. Benedek, *J. Chem. Phys.* **139**, 121904 (2013).

[47] P. R. ten Wolde and D. Frenkel, *Science* **277**, 1975 (1997).

[48] P. G. Vekilov, *J. Phys. Condens. Matter* **24**, 193101 (2012).

[49] A. Šarić, Y. C. Chebaro, T. P. J. Knowles, and D. Frenkel, *Proc. Natl. Acad. Sci. U.S.A.* **111**, 17869 (2014).

[50] A. J. Baldwin, P. Walsh, D. F. Hansen, G. R. Hilton, J. L. Benesch, S. Sharpe, and L. E. Kay, *J. Am. Chem. Soc.* **134**, 15343 (2012).

[51] M. P. Bova, L.-L. Ding, J. Horwitz, and B. K.-K. Fung, *J. Biol. Chem.* **272**, 29511 (1997).

[52] D. T. Humphreys, J. A. Carver, S. B. Easterbrook-Smith, and M. R. Wilson, *J. Biol. Chem.* **274**, 6875 (1999).

[53] P. Li, S. Banjade, H.-C. Cheng, S. Kim, B. Chen, L. Guo, M. Llaguno, J. V. Hollingsworth, D. S. King, S. F. Bannani, P. S. Russo, Q.-X. Jiang, T. B. Nixon, and M. K. Rosen, *Nature* **483**, 336 (2012).

[54] R. B. Griffiths and J. C. Wheeler, *Phys. Rev. A* **2**, 1047 (1970).

[55] A. D. Bruce and N. B. Wilding, *Phys. Rev. Lett.* **68**, 193 (1992).

[56] N. B. Wilding, *J. Phys. Condens. Matter* **9**, 585 (1997).

[57] W. M. Jacobs and D. Frenkel, *J. Chem. Phys.* **139**, 024108 (2013).